

Supporting Information:

**Driving Orbital Magnetism in Metallic
Nanoparticles through Circularly Polarized
Light: A Real-Time TDDFT Study**

Rajarshi Sinha-Roy,^{*,†} Jérôme Hurst,[¶] Giovanni Manfredi,^{*,§} and
Paul-Antoine Hervieux[§]

[†]*Aix-Marseille Univ, CNRS, CINaM, 13288 Marseille, France*

[‡]*European Theoretical Spectroscopy Facility (ETSF)*

[¶]*Univ. Grenoble Alpes, CNRS, CEA, Grenoble INP, IRIG-Spintec, 38000 Grenoble,
France*

[§]*Université de Strasbourg, CNRS, Institut de Physique et Chimie des Matériaux de
Strasbourg, UMR 7504, F-67000 Strasbourg, France*

E-mail: sinharoy@cinam.univ-mrs.fr; giovanni.manfredi@ipcms.unistra.fr

Ground state density

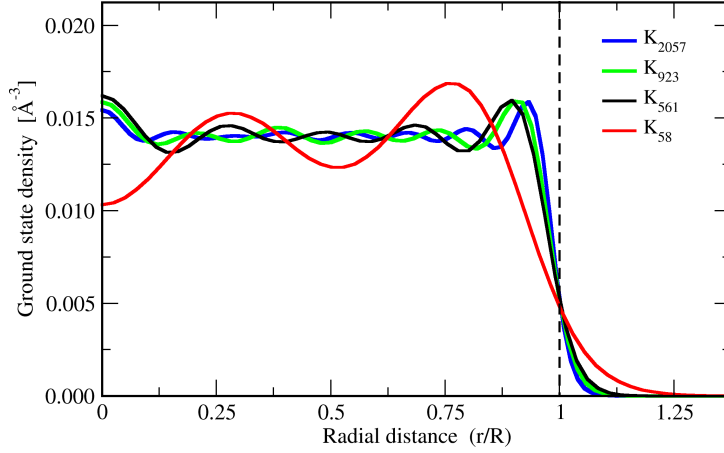


Fig. S1: Radial profiles of the ground-state electron density for Potassium clusters of different size.

In Fig. S1 we notice the effect of absolute size on the spill out of electron density with respect to the jellium boundary ($r/R = 1$). We also notice the quantum size-confinement effect: Friedel-like radial oscillation is present in the density profile in all the sizes presented in this figure. The spill-out becomes more and more important as we go down in size. The number of Friedel-like oscillation along the radial direction increases with the size.

Using Gaussian envelope for laser field

While in the manuscript we have used a sinusoidal envelope for the laser pulse, here in Fig. S2 we show the result of the calculation performed using a Gaussian envelope for the quasi-monochromatic circularly-polarized laser pulse for the jellium Au_{58} system. By choosing the the Gaussian envelope, the switching of the perturbation becomes much slower as compared to using the sinusoidal envelope. However, we can see that in comparison to the conclusions drawn upon the results presented in Fig. 2 of the manuscript, these results do not lead to any difference. As compared to Fig. 10 of the manuscript, (where we showed the dipole and magnetic moments in jellium Au_{58} due to a sinusoidal pulse,) the differences seen in these results (i.e., lower magnetic moment, and different

temporal evolution of the dipole moments) are solely due to the amount of energy transferred to the system which is smaller for the Gaussian pulse. However, these differences also do not affect our conclusions. The sinusoidal form of the envelope is enough to capture the physical effect we discussed in the manuscript through our results.

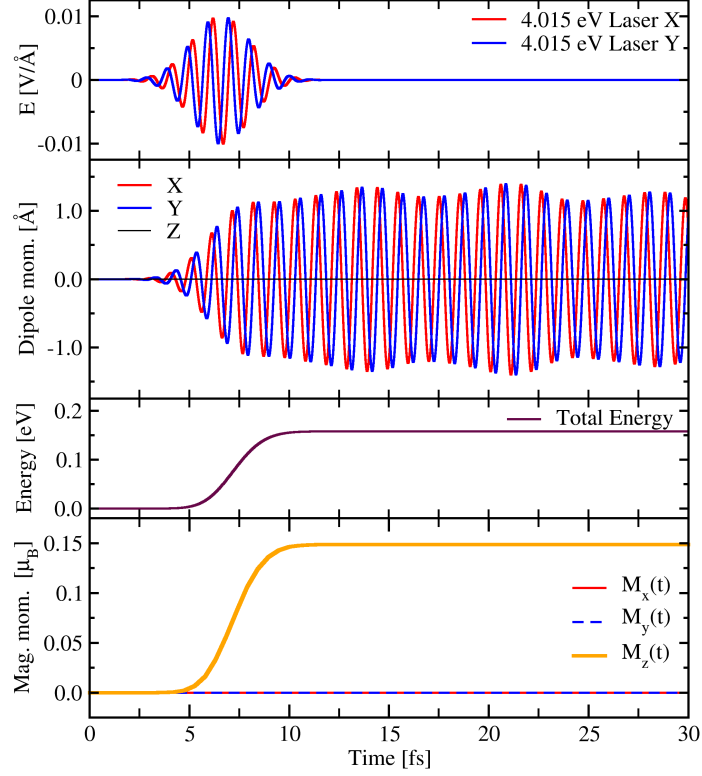


Fig. S2: Excitation of a jellium Au_{58} cluster with quasi-monochromatic circularly-polarized laser pulse at resonance energy (4.015 eV) and having a Gaussian temporal envelope. From top to bottom, the panels show the time dependence of the x (red) and y (blue) components of the laser electric field in $\text{V}/\text{\AA}$; the three components of the dipole moment in \AA ; the total energy absorbed by the electronic system in eV; and the three components of the magnetic moment, in units of the Bohr magneton μ_B .

K₅₆₁: Self-sustained dynamics of electrons

The time-dependent current density and induced density in Fig. S3 shows the dynamics of electrons during a full period of dipole oscillation. In this animation we notice that at a given instant of time the dipole moment and the current density are directed perpendicularly to each other. The induced density is directly proportional to the dipole moment and follows same sinusoidal time dependence. As the current is the rate of

Fig. S3: Animation showing the dynamics of electrons after laser is switched-off. **Top:** one full period of oscillation of the dipole moment in K_{561} highlighted in thick lines (x in red, y in blue). **Bottom:** the corresponding time-dependent induced density and current is shown respectively in the left and right panels. The blue circle represents the jellium boundary. The color code for the induced density and the arrowed representation for the current are the same as in the main article.

Acrobat pdf reader is required to see the animation.

change of charge density, because of the high symmetry of the system, it will also follow a sinusoidal variation in time out of phase with the time variation of induced density, i.e., of dipole moment. For this very reason, when the dipole moment is oriented along the y-direction (the beginning of the animation, at 15.16 fs), the current densities are directed towards the x-direction at most of the grid points within the cluster.

In this animation, we also notice that the phase lag (of rotation) between the different concentric contributions are present in both the induce density and the current. This is why in the animation we notice different circular paths of current at the interior of the cluster.

Jellium spheres with same radii

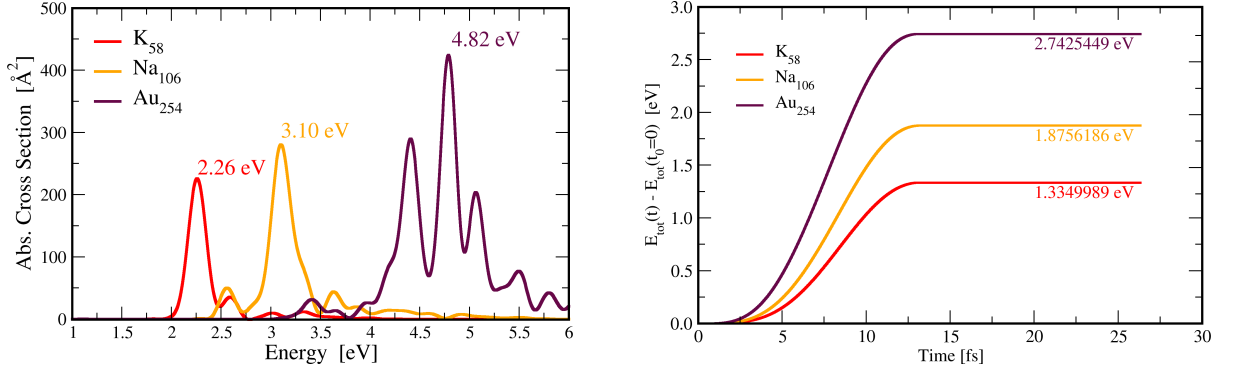


Fig. S4: **Left:** Absorption spectra of jellium spheres with almost the same jellium radius showing the most prominent features at 2.26 eV for K₅₈, at 3.10 eV for Na₁₀₆, and at 4.82 eV for Au₂₅₄. **Right:** The time dependence of energy (in eV) absorbed in K₅₈ (red), Na₁₀₆ (orange), and Au₂₅₄ (brown).

The LDA absorption spectra of jellium spheres K₅₈ ($r_s=2.57\text{\AA}$) with jellium radius 9.95Å, Na₁₀₆ ($r_s=2.083\text{\AA}$) with jellium radius 9.86Å, and Au₂₅₄ ($r_s=1.593\text{\AA}$) with jellium radius 10.08Å, showing the principal features upto 6 eV, are shown in the left panel of fig. S4. The most prominent features in the spectra are at 2.26 eV for K₅₈, at 3.10 eV for Na₁₀₆, and at 4.82 eV for Au₂₅₄. The systems have resonant response at these energies. Thus they are excited at those energies with a circularly polarized laser in order to study the corresponding response. The right panel of fig. S4 shows the total energy absorbed in those systems.

Jellium spheres with same number of electrons

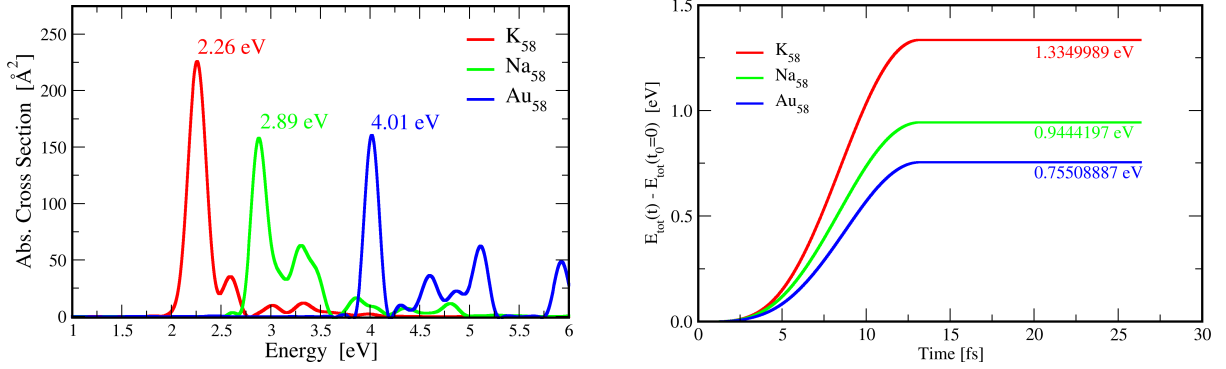


Fig. S5: **Left:** Absorption spectra of jellium spheres having same number of electrons, showing the most prominent features at at 2.26 eV for K₅₈, at 2.89 eV for Na₅₈, and at 4.01 eV for Au₅₈. **Right:** The time dependence of energy (in eV) absorbed in K₅₈ (red), Na₅₈ (green), and Au₅₈ (blue).

Fig. S5: The LDA absorption spectra of jellium spheres K₅₈ ($r_s=2.57\text{\AA}$) with jellium radius 9.95Å, Na₅₈ ($r_s=2.083\text{\AA}$) with jellium radius 8.06Å, and Au₅₈ ($r_s=1.593\text{\AA}$) with jellium radius 6.165Å, showing the principal features upto 6 eV, are shown in the left panel of fig. S5. The most prominent features in the spectra are at 2.26 eV for K₅₈, at 2.89 eV for Na₅₈, and at 4.01 eV for Au₅₈. The systems have resonant response at these energies. Thus they are excited at those energies with a circularly polarized laser in order to study the corresponding response. The right panel of fig. S5 shows the total energy absorbed in those systems.

Normalized magnetic moment per atom

Normalized magnetic moments per-atom calculated for jellium gold spheres (Au_{254} , and Au_{58}) are compared with the experimental results of Cheng et al.¹ in Table T1.

Table T1: Per-atom magnetic moment normalized with respect to laser intensity and pulse-width compared for Au.

System	$N_{\text{atom}},$ Rad. [Å]	r_s [Å]	ω [eV]	T [fs]	I_0 $\left[\frac{\text{W}}{m^2} 10^{13}\right]$	M_z [μ_B]	m [μ_B] or $M_z/N_{\text{at.}}$ [μ_B]	$m' = \frac{m}{I_0 T}$ $\left[\frac{\mu_B m^2}{\text{fs W}} 10^{-17}\right]$
Ref.[1]	$\sim 3.1 \times 10^7,$ 500	1.5916	2.41	370	9.09		0.949	2.82163
Au_{254}	254, 10.08	1.5928	4.82	13.16	1.327	2.18	0.00858	4.91315
Au_{58}	58, 6.615	1.5928	4.01	13.16	1.327	0.71	0.01233	7.06051

References

- (1) Cheng, O. H.-C.; Son, D. H.; Sheldon, M. Light-induced magnetism in plasmonic gold nanoparticles. *Nature Photonics* **2020**, *14*, 365–368.